Article

Sustainability assessment of highly fluorescent Carbon Dots derived from Eucalyptus Leaves

Archana Johny , Luís Silva , Carlos Pereirs , Joaquim C. G. Esteves da Silva *

Posted Date: 6 July 2023

doi: 10.20944/preprints202307.0424.v1

Keywords: Carbon dots; green synthesis; biomass; eucalyptus leaves; high quantum yield; life cycle assessment

Article

Sustainability Assessment of Highly Fluorescent Carbon Dots Derived from Eucalyptus Leaves

Archana Johny [1], Luís Pinto da Silva [2], Carlos M. Pereira [1], Joaquim C. G. Esteves da Silva [2, *]

[1] Chemistry Research Unit (CIQUP), Institute of Molecular Sciences (IMS), Department of Chemistry and Biochemistry, Faculty of Sciences, University of Porto, Rua do Campo Alegre s/n, 4169-007 Porto, Portugal; archanajohny@gmail.com; cmpereir@fc.up.pt

[2] Chemistry Research Unit (CIQUP), Institute of Molecular Sciences (IMS), Department of Geosciences, Environment and Territorial Planning, Faculty of Sciences, University of Porto, Rua do Campo Alegre s/n, 4169-007 Porto, Portugal; luis.silva@fc.up.pt

* Correspondence: jcsilva@fc.up.pt

Abstract: Biomass-derived carbon dots (CDs) are gaining much interest in recent times as it is a sustainable option with abundant availability, low cost, and tunable luminescence. Herein, we report a simple green synthesis method to produce highly fluorescent CDs from *Eucalyptus globulus* leaves using the one-pot hydrothermal approach. The fabricated CDs exhibit strong blue fluorescence with an excitation and emission maxima of 340 nm and 442 nm respectively. The highest quantum yield (QY) obtained was 60.7%. Due to its promising optical properties and biocompatibility, CDs can be a potential candidate for biosensing applications. Moreover, we employed a life cycle assessment (LCA) cradle-to-gate approach to study the environmental impacts of the synthesis strategy used for the fabrication of CDs. The results point out that citric acid is a main hotspot in CDs synthesis, regarding environmental impacts in most categories. This justifies the introduction of biomass, which reduces the amount of citric acid, thus leading to a more sustainable synthesis strategy for fabricating CDs.

Keywords: carbon dots; green synthesis; biomass; eucalyptus leaves; high quantum yield; life cycle assessment

1. Introduction

CDs are fluorescent spherical carbon nanomaterials with particle size typically less than 10 nm, discovered in 2004 by Xu *et al*. [1] and named in 2006 by Sun *et al*. [2]. They possess excellent properties such as adjustable emission wavelength, easy surface modification, low cytotoxicity, good biocompatibility, photostability and excellent water stability, among others [3]. Multiple methods are available for the synthesis of CDs and are mainly classified into two main synthesis routes: Top-down and Bottom-up methods [4]. Top-down approaches involve the exfoliation of large pure carbon compounds like carbon black, carbon nanotubes or graphite into nanoscale CDs. These methods are relatively expensive and require complex steps and harsh experimental conditions [3]. Laser ablation [5], electrochemical oxidation [6], chemical oxidation [7], etc, are examples of top-down methods. The bottom-up approaches like hydrothermal method [8], microwave-assisted methods [9], solvothermal methods [10], pyrolysis [11], etc, convert small organic molecules or biological carbon materials like biomass waste or plant and animal products into carbon dots via carbonization and passivation [3]. The bottom-up methods are thus more advantageous in the sense that they are cost effective, environment friendly, and simple surface modification can be achieved in one-pot [12].

CDs synthesized from biomass are nowadays becoming one of the research hotspots in application fields such as sensing [13], imaging [14], drug delivery [15], photocatalysis [16] etc, due to various advantages including easy availability of carbon source, simplicity in preparation and feasibility of large-scale production. Biomass waste is a natural organic carbon source mainly composed of cellulose, hemicellulose, lignin, ash, proteins, etc, [3]. For example, in the case of plant biomass, cellulose accounts for 30-60%, hemicellulose 20-40% and lignin 15-25% [17]. Hence, it is useful to utilize biomass waste as raw materials to produce CDs. Another important aspect about CDs from biomass waste is the possibility of self-passivation during the synthetic process itself due

 doi:10.20944/preprints202307.0424.v1

to the presence of heteroatoms containing compounds which can act as self-passivating agents [3]. Examples of biomass derived CDs reported in literature are from sources like spent coffee grounds [18], green tea leaf [19], *Pyrus pyrifolia* fruit [20], papaya waste pulp [21], banana peel [22], willow catkin [23], Chionantus retusus fruit extract [24], bamboo leaf [25], orange juice [26], Seville orange [27], starch fermentation wastewater [28], mango peel [29], among others.

Haghani *et al* used eucalyptus leaves for the first time as carbon dots precursor for an optical sensor application based on molecular imprinting technique [30]. *Eucalyptus globulus* is the main eucalyptus species cultivated in Portugal and is characterized by high productivity [31]. Due to its richness in hydrocarbon groups and abundant availability, Eucalyptus leaves can be an excellent choice as the carbon precursor for CDs synthesis [32]. However, the most common precursors used for the preparation of CDs are citric acid as carbon source and amine containing molecules as the nitrogen source, as nitrogen doping is indicated to be an efficient strategy to enhance photoluminescence [33–35]. In this paper, we discuss the green synthesis of nitrogen doped CDs based on *Eucalyptus globulus* leaves and citric acid with high quantum yield. We also evaluate the environmental impacts of the synthesis strategy using the LCA approach.

LCA is an important tool for sustainable development. As the name indicates, LCA is a methodology for the systematic analysis of the potential environmental impacts of a product (or service) during their entire life cycle from cradle to grave, ie; raw material extraction, transportation, production, distribution, use, and end of life phases [36]. LCA studies have been already employed to study the environmental impacts of CDs like for the comparative study of different bottom-up procedures for the fabrication of CDs [37–39]. With this study, we expect to identify the most critical parameters giving rise to environmental impacts. Given this, we expect to provide a basis for future studies to design a cleaner strategy for the high-yield production of CDs.

2. Materials and Methods

2.1. Materials

Eucalyptus leaves (*Eucalyptus globulus*) were collected from local plantations in Portugal. Citric acid (anhydrous, ≥99.5%) and Ethylenediamine (≥99%) were purchased from Sigma-Aldrich (St. Louis, MO, USA). Quinine sulphate dihydrate from VWR Chemicals BDH®, (Leuven, Belgium) and Sulphuric acid from Merck were used for QY calculations. The dialysis membranes with molecular weight cut-off 1000 Da were from Float-A-Lyzer®G2 Dialysis Device SPECTRUM® (New Brunswick, NJ, USA).

2.2. Instrumentation

Fluorescence spectra were obtained in a standard 10 mm fluorescence quartz cell and collected in Horiba Jobin Yvon Fluoromax-4 spectrofluorometer. The absorption measurements were made with Jasco V-760 UV- visible spectrophotometer. Attenuated total reflectance - Fourier Transform Infrared Spectroscopy (ATR-FTIR) measurements were performed in the range of 600 – 4000 cm^{-1} using spectrophotometer Bruker FT-IR System Tensor 27 with diamond ATR crystal. The pH of the buffer solution was adjusted using a pH meter. Atomic force microscopy (AFM) analysis was carried out using Veeco Metrology Multimode/Nanoscope IVA by tapping mode, using a Bruker silicon probe (model TESP-SS, resonant frequency 320 kHz, nominal force constant 42 N/m, estimated tip radius 2 nm). X-ray diffraction (XRD) analysis was performed by SmartLab Rigaku Diffractometer (Cu-Kα radiation) with a θ=2θ scanning equipment and using the Bragg Brentano (BB) geometry. Raman spectrum was measured with a Renishaw inVia Raman microscope coupled with 633 nm 17 mW (He–Ne) and 785 nm 300 mW (diode) lasers.

2.3. Preparation of CDs

Eucalyptus leaves were used as the main carbon source and ethylenediamine as the nitrogen dopant in a single step hydrothermal method for the synthesis of carbon dots as illustrated in the Figure 1. Firstly, Eucalyptus leaves were carefully rinsed with distilled water to remove any

Preprints (www.preprints.org) | NOT PEER-REVIEWED | Posted: 6 July 2023 doi:10.20944/preprints202307.0424.v1

contamination or dirt and then dried at room temperature. Next, it was milled to obtain a fine powder of 112 μm size.

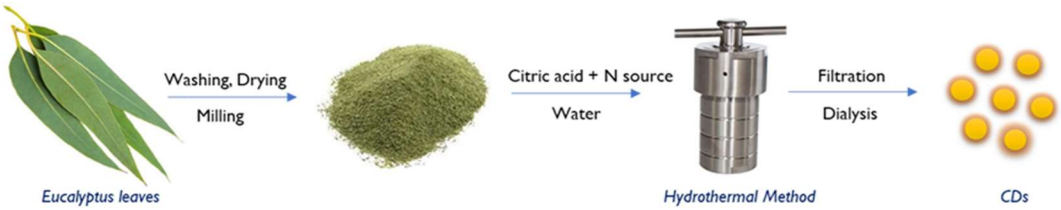

Figure 1. Schematic representation of synthesis of CDs from Eucalyptus leaves.

The optimum proportion of the reagents (eucalyptus power, citric acid and ethylenediamine) and experimental factors (temperature and time) to obtain the highest quantum yield (QY) was obtained using a multivariate experimental design strategy using Unscramble Design v9.6 (CAMO Software AS, Oslo, Norway) using a sequence of designs.

The optimum experimental factors were: 1 g of powdered eucalyptus leaves and 1 g of citric acid were added to 40 mL of distilled water; followed by the addition of 863 μL of ethylenediamine; adjusting the pH to 9.5; the mixture was transferred into the stainless-steel autoclave and kept in a hot air oven at 180^{0}C for 24 hrs. As a result, a dark brown solution was obtained. After that it was centrifuged at 6000 rpm for 30 min to remove larger particles and non-fluorescent particles. A clear brown coloured solution is collected and filtered using 0.45 μm membrane filter paper. The product was purified by using dialysis bags of MWCO 1000 Da for about 48 hrs. The purified CDs obtained are then lyophilized in a freeze dryer for 48 hrs to produce brownish powder form and stored at 4^{0}C. The average synthesis yield was calculated to be 1.95% by considering the final weight of powder obtained relative to the initial weight of precursor(s) used in powder form.

2.4. Quantum yield measurements

Fluorescence quantum yield (QY) was calculated with a standard procedure, based on the comparison of the integrated luminescence intensities and absorbance values of the synthesised CDs with a reference (which depends on the emission wavelength of the sample) quinine sulphate with the following equation:

$$QY_{FL}^{Sample} = QY_{FL}^{Reference} \times \frac{Grad_{Sample}}{Grad_{Reference}} \times \frac{\eta_{Sample}^2}{\eta_{Reference}^2} \quad (1)$$

where Grad is the gradient from the plot of integrated fluorescence intensity versus absorbance and the refractive index. Quinine sulphate was chosen as a reference fluorophore of known quantum yield (QY = 0.54) [35].

2.4. Environmental impact assessment

The environmental impacts assessment associated with the synthesis of CDs was based on inventory data from laboratory-scale synthesis procedures described on Section 2.3. The life cycle inventory data for the foreground system of the synthesis procedure consists of different processes and chemicals included in this study and were modelled with the following data present in the Ecoinvent® 3.5 database (GLO standing for global, RER for regional market for Europe, and PT for Portugal) as described in Table 1. Eucalyptus was not included in the simulation model directly unlike the commercial reagents, electricity produced and treated water, as we are using this biomass as an effort to reduce the amount of commercial reagents. So, our focus was on assessing the environmental impacts associated with lowering the amount of used citric acid.

 doi:10.20944/preprints202307.0424.v1

Table 1. Data inventory used from Ecoinvent® 3.5 database.

Denomination	Proposed correspondence in Ecoinvent® 3.5 database
Citric acid	Citric acid {GLO}| market for | Cut-off, S
Ethylenediamine	Ethylenediamine {RER}| production | Cut-off, S
Electricity	Electricity, medium voltage {PT}| market for | Cut-off, S
Deionized water	Water, deionised, from tap water, at user {Europe without Switzerland} | market for water, deionised, from tap water, at user | Cut-off, S

The present LCA study is based on a cradle-to-gate approach, from the production of precursor materials to the fabrication of CDs. Environmental impacts were modelled using the ReCiPe 2016 v1.1 midpoint method, Hierarchist version [40]. The impact potentials evaluated according to the ReCiPe method were: global warming (GW), stratospheric ozone depletion (SOD), ionizing radiation (IR), ozone formation-human health (OF-HH), fine particulate matter formation (FPM), ozone formation-terrestrial ecosystem (OF-TE), terrestrial acidification (TA), freshwater eutrophication (FE), marine eutrophication (ME), terrestrial ecotoxicity (TET), freshwater ecotoxicity (FET), marine ecotoxicity (MET), human carcinogenic toxicity (HCT), human non-carcinogenic toxicity (HNCT), land use (LU), mineral resource scarcity (MRS), fossil resource scarcity (FRS), water consumption (WC). The LCA study was performed by using the SimaPro9 software.

3. Results and Discussion

3.1. Surface morphology

AFM measurements were performed to study the morphology of CDs and specially to ensure that the particles are indeed nanosized. Figure 2(a) shows the AFM image of the CDs, and the average particle size was determined to be 6 ± 2 nm. FTIR spectroscopy was used to analyse the surface functional groups present in the CDs. As evident from the spectrum Figure 2(b), the broad characteristic peak around 3232 cm^{-1} refers to the stretching vibrations of N-H or O-H bonds. The absorbance band at 2927 cm^{-1} indicates the C-H stretching vibration [30]. The sharp peaks at 1555 cm^{-1} and 1384 cm^{-1} correspond to the stretching vibration of the COO^- and C–H groups respectively [41]. The aliphatic C-N stretching vibration is ascribed to the peak at 1264 cm^{-1}. Besides, the absorption bands ranging from 1200 to 1000 cm^{-1} can be attributed to the C–O–C groups. The N–H deformation vibration is observed at 831 cm^{-1} [42]. The FTIR signals demonstrate that CDs possessed various hydrophilic functional groups containing hydroxyl, amino, and carboxyl groups which are beneficial to further strengthen the water solubility and fluorescent properties of the as-prepared CDs [43].

Preprints (www.preprints.org) | NOT PEER-REVIEWED | Posted: 6 July 2023 doi:10.20944/preprints202307.0424.v1

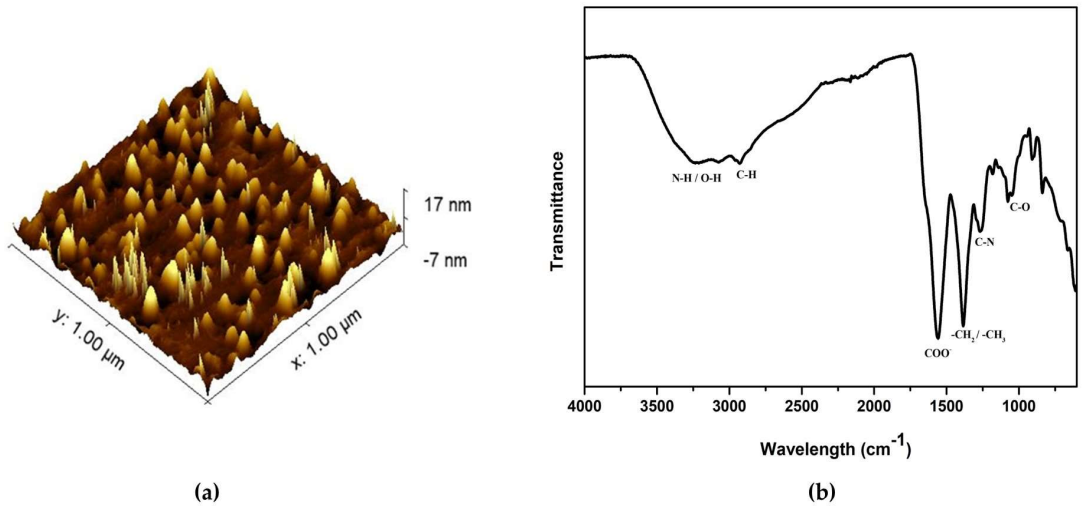

Figure 2. (a) AFM image of CDs; (b) FTIR spectra of CDs**.**

To study the surface composition and electronic states of the elements present in CDs, XPS analysis was conducted, and the results are shown in Figure 3(a). It shows three major peaks of C 1s, N 1s and O 1s at 285, 400 and 532.4 eV respectively. Si 2s and Si 2p peaks were also present due to the most common silica contamination and hence were not taken to account for detailed analysis. The content of C, N and O (in %) was 67.3, 10.7 and 22 %, respectively.

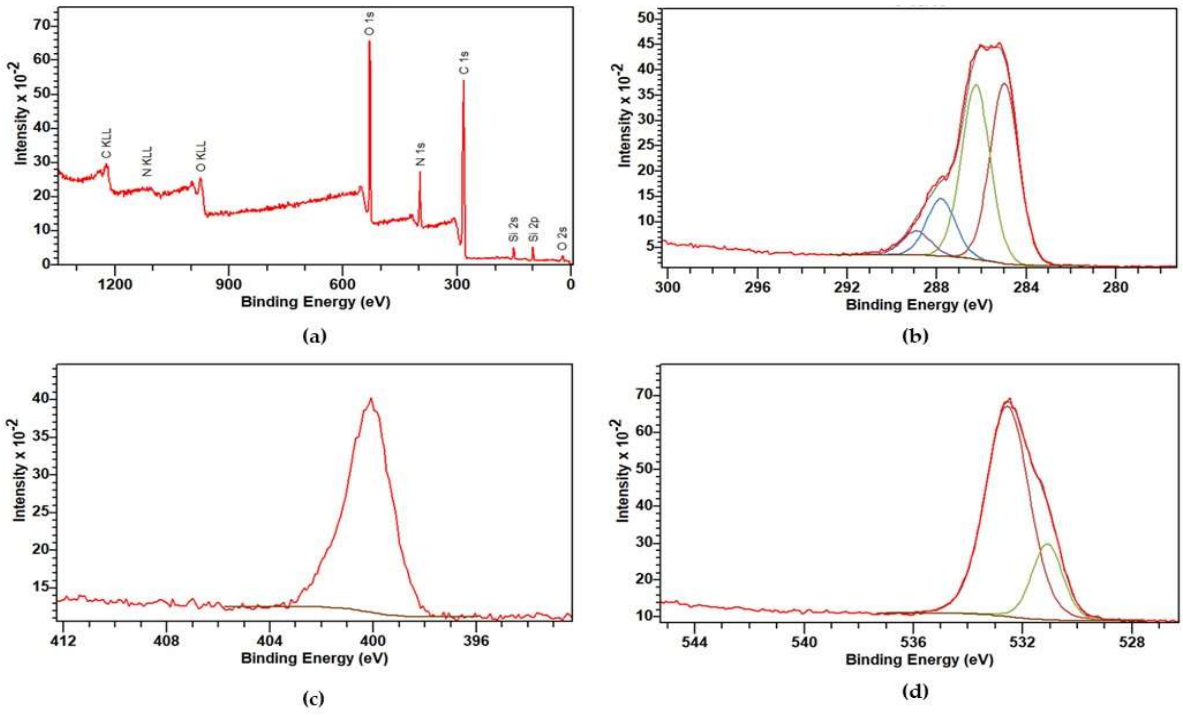

Figure 3. XPS: **(a)** full survey spectrum of CDs; High resolution XPS of the: **(b)** C 1s; **(c)** N 1s; and **(d)** O 1s.

A detailed scan was performed for the C 1s, O 1s and N 1s internal levels for deconvolution, chemical state, and the quantitative analysis. The C 1s spectrum displays four distinct peaks at 284.9 eV (41.25 %), 286.2 eV (40.01 %), 287.8 eV (13.23 %) and 288.9 eV (5.51 %) as shown in Figure 3(b). These peaks can be attributed to C–C / C=C bond (284.9 eV), C–N bond (286.2 eV), O–C=O / C=N bond (287.8 eV) and C=O bond (288.9 eV) respectively[44,45]. As given in Figure 3(c), N 1s core level spectrum shows only one peak at 400 eV which can be ascribed to the N-H group [45]. The

Preprints (www.preprints.org) | NOT PEER-REVIEWED | Posted: 6 July 2023 doi:10.20944/preprints202307.0424.v1

deconvolution of O 1s spectrum shown in Figure 3(d) yielded a major peak at 532.5 eV (79.56%) due to C-O linkage, with a relatively small contribution at 531 eV (20.44%) representing C=O functional group [46]. The results are in good agreement with FTIR results.

XRD spectra in Figure 4(a) reveals a weak broad peak around $2\theta=24^0$ corresponding to (002) hkl plane (JCPDS card no. 26-1076). The interplanar distance (002) is calculated to be 0.37 nm which is slightly higher than the graphitic interlayer spacing. XRD results show the poor crystalline nature of CDs [47].

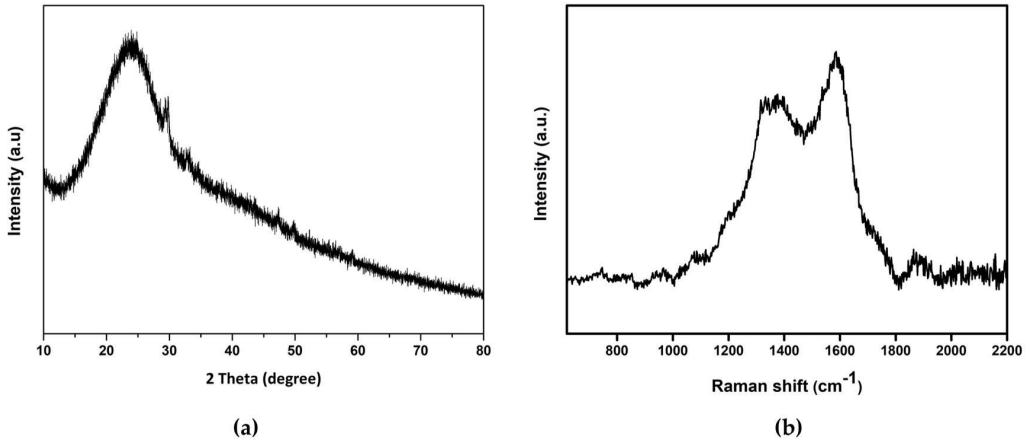

Figure 4. (a) XRD spectra of CDs; **(b)** Raman spectra of CDs.

The Raman spectrum is shown in Figure 4(b), both spectra exhibit two broad features, at 1367 cm^{-1} and 1585 cm^{-1}, close to the D (disorder) and G (graphite) bands, respectively. D band corresponds the vibrations of carbon atoms with dangling bonds in the termination plane of disordered graphite or glassy carbon, while the G band is related to E_{2g} mode of the graphite and the vibration of sp^2 bonded carbon atoms in a two-dimensional hexagonal lattice. The intensity of G band is higher than D band indicating there are principally sp^2 carbons with some sp^3 hybrid carbons in carbon dots [48,49]. Thus, carbon dots are mainly composed of sp^2 graphitic carbons with sp^3 carbon defects. This indicates the amorphous nature of the synthesized CDs.

3.2. Optical properties

In the UV-Vis absorption spectrum of CD in Figure 5(a) reveals two absorption bands. The peak at 285 nm is due to $\pi-\pi^*$ transition of C=C bonds in sp^2 hybridised domain of the graphitic core, which do not usually generate fluorescence [50,51]. However, the peak at 345 nm is attributed to $n-\pi^*$ transition of C=O, C–N or C–OH bonds in the sp^3 hybridised domains, which can be originated from carboxyl (–COOH) or amine ($-NH_2$) groups existing on the surface of CDs. This is supposed to have a more prominent impact on the photoluminescence properties of the CDs [52]. The fluorescence of CDs upon the UV irradiation at 365 nm is represented in Figure 5(b). Very bright blue luminescence was observed under the illumination of UV (365 nm) light.

Preprints (www.preprints.org) | NOT PEER-REVIEWED | Posted: 6 July 2023 doi:10.20944/preprints202307.0424.v1

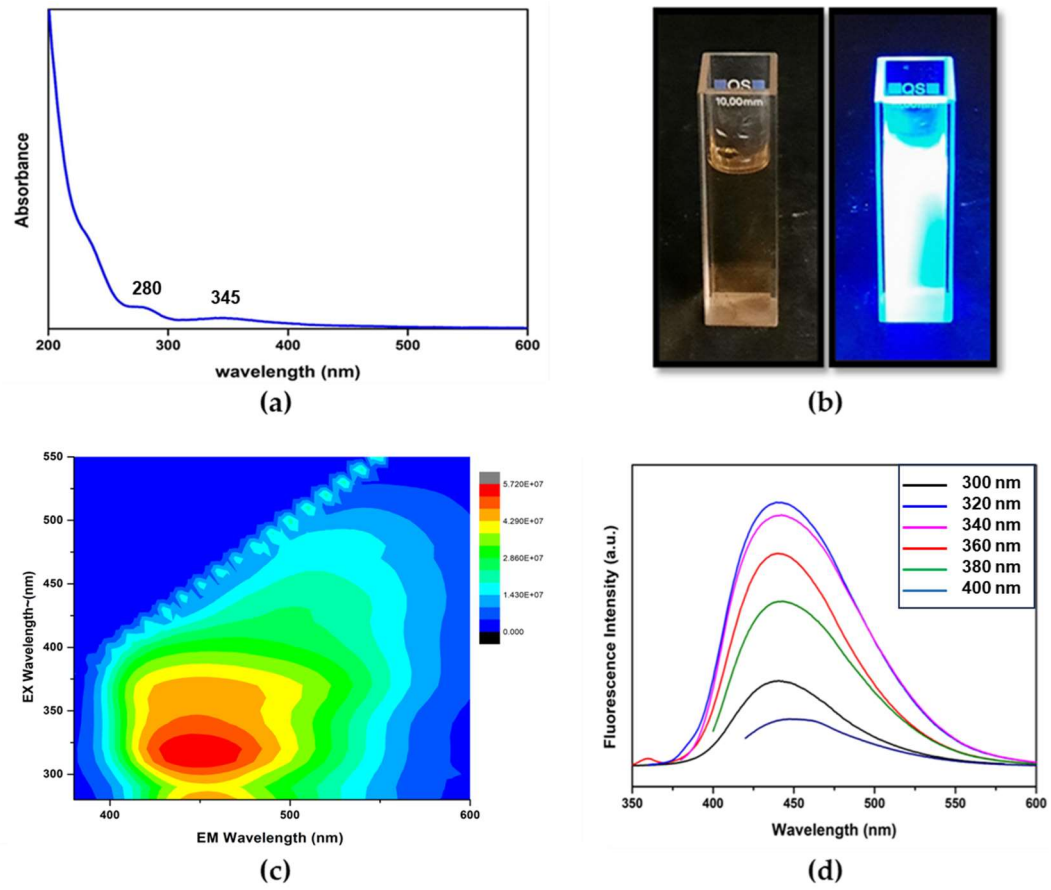

Figure 5. (a) UV-visible spectrum of CDs in aqueous solution; **(b)** CDs in aqueous solution before and after UV irradiation; **(c)** 2D excitation-emission contour plot; **(d)** Excitation independent Emission fluorescence spectra of CDs in aqueous solution.

The optical properties of the CDs were further studied using fluorescence spectrometry. From the fluorescence 2D contour plot of CDs in Figure 5(c), the maximum excitation and emission wavelength of CDs were found to be around 320 nm and 445 nm respectively. As indicated in Figure 5(d), the CDs clearly show an excitation independent emission throughout the range of 300-400 nm. Usually, excitation-dependent FL behaviors of CDs reflect effects from particles of different sizes in sample and a distribution of different surface states [53]. Clearly from the AFM image given in Figure 2(a), it is evident that there is a size distribution in the CDs. Therefore, the excitation-independent FL behavior suggests that the FL properties of the CDs are dependent on the surface states rather than the morphology. Hence, the surface states of the CDs should be rather uniform. Using Quinine Sulphate as a reference (QY = 54%, λ_{ex} = 350 nm), the relative quantum yield (QY) of CDs was measured to be 60.7%. As compared to the QY ranging from 8.5%-31.7% for the reported CDs derived from other biomass sources given in Table 2, Eucalyptus CDs has relatively high QY of 60.7%.

Table 2. Synthesis methods, conditions, quantum yields, maximum excitation and emission wavelengths of various biomass derived CDs.

Biomass source	Synthesis Method	Conditions	QY (%)	$\lambda_{ex}/\lambda_{em}$ (nm)	Ref.
Green tea leaf	Pyrolysis, oxidation	2h of pyrolyzation	14.8%	320/410	[19]

Preprints (www.preprints.org) | NOT PEER-REVIEWED | Posted: 6 July 2023 doi:10.20944/preprints202307.0424.v1

		at 350°C, 20h of oxidation			
Pyrus pyrifolia fruit	Hydrothermal	180°C, 6h	10.8%	390/471	[20]
Carica papaya waste pulp	Pyrolysis	200°C, 15 min	23.7%	310/462	[21]
Dwarf banana peel	Hydrothermal	200°C, 24h	23%	345/445	[22]
Willow catkin	Combustion	Dried at 80°C and burned to ashes	13.3%	310/370	[23]
Chionanthus retusus fruit extract	Hydrothermal	180°C, 6h	9%	340/425	[24]
Bamboo leaf	Calcination	300°C, 3h	5.18%	313/419	[25]
Orange juice	Hydrothermal	200°C, 11h	31.7%	360/449	[26]
Seville Orange	Hydrothermal	130°C, 12h	13.3%	330/402	[27]
Starch fermentation wastewater	Hydrothermal	180°C, 10h	24.5%	460/518	[28]
Mango peel	Pyrolyzation with oxygenolysis	300°C, 6h	8.5%	310/425	[29]
Eucalyptus leaves	Hydrothermal	180°C, 24h	60.7%	320/445	This work

The fluorescence lifetime analysis spectra of CDs given in Figure 6 was obtained using a biexponential fitting. The lifetime decay of CDs fits (with a $\chi^2 = 1.24$) the two-fluorophores model giving the average lifetimes of 4.29 ± 0.2 ns and 15.12 ± 0.02 ns with the pre-exponential factors A = 11.4 ± 0.2, B1 = $7.41\times10^{-3} \pm 8\times10^{-5}$, and B2 = $3.52\times10^{-2} \pm 3\times10^{-5}$.

Preprints (www.preprints.org) | NOT PEER-REVIEWED | Posted: 6 July 2023 doi:10.20944/preprints202307.0424.v1

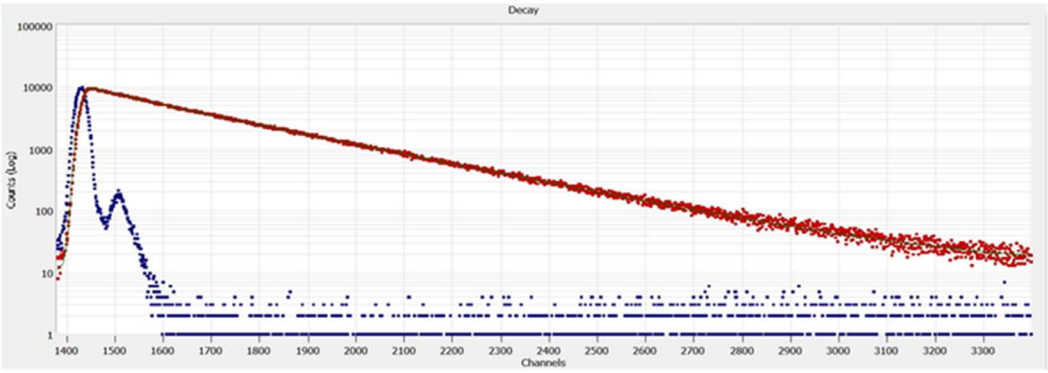

Figure 6. Fluorescence lifetime analysis spectra of CDs.

3.3. Life cycle Assessment

LCA study was carried out to understand the environmental impacts of the hydrothermal synthesis under study using a weight based functional unit of 1 kg of CDs. The method ReCiPe 2016 Midpoint, Hierarchist version was followed, and the results obtained are shown in Figure 7. The objective of this study is not to make quantitative appreciations of the environmental impacts of each material input, but to compare the contributions to the different impact categories of the input involved in this synthesis.

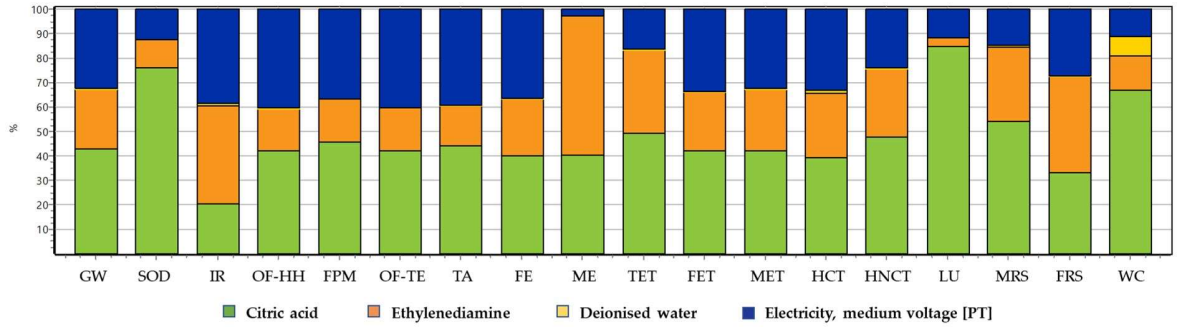

Figure 7. Environmental impacts analysis of hydrothermally synthesized CDs with the ReCiPe 2016 Midpoint (H). Abbreviations are explained under Section 2.4.

From the results of the analysis, it is evident that citric acid is the resource with major contributions (between 20 and 85%) when compared to other resources in almost all environmental impact categories. The contribution of citric acid is quite higher in the categories of land use (85%) and stratospheric ozone depletion (76.2%). The only exceptions are the categories of ionizing radiation, marine eutrophication, and fossil resource scarcity where ethylenediamine is the major contributor with 40, 56.9 and 39.4% respectively. After ethylenediamine, electricity is another important resource with significant contributions up to 40.6% in most categories except marine eutrophication (2.79%). However, deionized water does not appear to have any relevant environmental impact, when comparing with the other resources, even in the categories related with water consumption.

In general, the carbon precursor used for bottom-up synthesis of CDs being the main hotspot with higher associated environmental impacts, followed by electricity being another significant contributing parameter, is in line with the existing literature [38,39].

Based on the results of LCA, citric acid is the major hotspot in most of the environmental impact categories evaluated in this study. It can be deduced that a more sustainable synthetic route was adopted for the synthesis of CDs by using biomass as a precursor, as it reduced the amount used of citric acid. Otherwise, the environmental impacts would have been expected to be relevantly higher, by doubling the amount used for the main hotspot.

4. Conclusion

In summary, Eucalyptus leaves have proved to be a good candidate for bioinspired preparation of carbon dots with blue fluorescence and high quantum yield. The preparation methods are easy and environmentally friendly. LCA studies also support the idea of inclusion of biomass in this hydrothermal synthesis route by showing that commercial carbon precursor, citric acid, is still the main responsible for environmental impacts. High quantum yield of around 60.7% was able to be achieved. Since CDs exhibit good solubility in water and superior fluorescent properties, they can be potentially explored for various applications in the fields of sensing, bioimaging, photocatalysis, drug delivery etc.

Funding: This research was funded by 'Fundação para a Ciência e Tecnologia' (FCT), Portugal, grant number UI/BD/151340/2021. We also acknowledge FCT for funding the R&D Unit CIQUP (UIDB/000081/2020 and UIDP/00081/2020), the Associated Laboratory IMS (LA/P/0056/2020), and L.P.S. (CEECINST/00069/2021).

Data Availability Statement: The data presented in this study are available on request from the corresponding author.

Acknowledgments: The authors wish to acknowledge Joaquim Agostinho Moreira's group from Institute of Physics for Advanced Materials, Nanotechnology and Photonics (IFIMUP), Physics and Astronomy Department, FCUP (Porto, Portugal) for using their excellent Raman facility (Renishaw spectrometer).

Conflicts of Interest: The authors declare no conflict of interest.

References

1. X. Xu *et al.*, 'Electrophoretic Analysis and Purification of Fluorescent Single-Walled Carbon Nanotube Fragments', *J. Am. Chem. Soc.*, vol. 126, no. 40, pp. 12736–12737, Oct. 2004, doi: 10.1021/ja040082h.
2. Y.-P. Sun *et al.*, 'Quantum-Sized Carbon Dots for Bright and Colorful Photoluminescence', *J. Am. Chem. Soc.*, vol. 128, no. 24, pp. 7756–7757, Jun. 2006, doi: 10.1021/ja062677d.
3. C. Kang, Y. Huang, H. Yang, X. F. Yan, and Z. P. Chen, 'A Review of Carbon Dots Produced from Biomass Wastes', *Nanomaterials*, vol. 10, no. 11, p. 2316, Nov. 2020, doi: 10.3390/nano10112316.
4. J. C. G. Esteves Da Silva and H. M. R. Gonçalves, 'Analytical and bioanalytical applications of carbon dots', *TrAC Trends in Analytical Chemistry*, vol. 30, no. 8, pp. 1327–1336, Sep. 2011, doi: 10.1016/j.trac.2011.04.009.
5. D. Reyes *et al.*, 'Laser Ablated Carbon Nanodots for Light Emission', *Nanoscale Research Letters*, vol. 11, no. 1, 2016, doi: 10.1186/s11671-016-1638-8.
6. Y. Hou, Q. Lu, J. Deng, H. Li, and Y. Zhang, 'One-pot electrochemical synthesis of functionalized fluorescent carbon dots and their selective sensing for mercury ion', *Analytica Chimica Acta*, vol. 866, pp. 69–74, Mar. 2015, doi: 10.1016/j.aca.2015.01.039.
7. Z.-A. Qiao *et al.*, 'Commercially activated carbon as the source for producing multicolor photoluminescent carbon dots by chemical oxidation', *Chem. Commun.*, vol. 46, no. 46, pp. 8812–8814, Nov. 2009, doi: 10.1039/C0CC02724C.
8. K. Qu, J. Wang, J. Ren, and X. Qu, 'Carbon Dots Prepared by Hydrothermal Treatment of Dopamine as an Effective Fluorescent Sensing Platform for the Label-Free Detection of Iron(III) Ions and Dopamine', *Chemistry – A European Journal*, vol. 19, no. 22, pp. 7243–7249, 2013, doi: 10.1002/chem.201300042.
9. X. Wang, K. Qu, B. Xu, J. Ren, and X. Qu, 'Microwave assisted one-step green synthesis of cell-permeable multicolor photoluminescent carbon dots without surface passivation reagents', *J. Mater. Chem.*, vol. 21, no. 8, pp. 2445–2450, Feb. 2011, doi: 10.1039/C0JM02963G.
10. Z. Lu *et al.*, 'Potential Application of Nitrogen-Doped Carbon Quantum Dots Synthesized by a Solvothermal Method for Detecting Silver Ions in Food Packaging', *International Journal of Environmental Research and Public Health*, vol. 16, no. 14, Art. no. 14, Jan. 2019, doi: 10.3390/ijerph16142518.
11. J. Qin, L. Zhang, and R. Yang, 'Solid pyrolysis synthesis of excitation-independent emission carbon dots and its application to isoniazid detection', *J Nanopart Res*, vol. 21, no. 3, p. 59, Mar. 2019, doi: 10.1007/s11051-019-4503-8.
12. D. Ozyurt, M. A. Kobaisi, R. K. Hocking, and B. Fox, 'Properties, Synthesis, and Applications of Carbon Dots: A Review', *Carbon Trends*, p. 100276, Jun. 2023, doi: 10.1016/j.cartre.2023.100276.
13. M. Abdullah Issa *et al.*, 'Facile Synthesis of Nitrogen-Doped Carbon Dots from Lignocellulosic Waste', *Nanomaterials*, vol. 9, no. 10, p. 1500, Oct. 2019, doi: 10.3390/nano9101500.

14. R. Atchudan, T. N. Jebakumar Immanuel Edison, M. Shanmugam, S. Perumal, T. Somanathan, and Y. R. Lee, 'Sustainable synthesis of carbon quantum dots from banana peel waste using hydrothermal process for in vivo bioimaging', *Physica E: Low-dimensional Systems and Nanostructures*, vol. 126, p. 114417, Feb. 2021, doi: 10.1016/j.physe.2020.114417.
15. T. S. John, P. K. Yadav, D. Kumar, S. K. Singh, and S. H. Hasan, 'Highly fluorescent carbon dots from wheat bran as a novel drug delivery system for bacterial inhibition', *Luminescence*, vol. 35, no. 6, pp. 913–923, Sep. 2020, doi: 10.1002/bio.3801.
16. D. S. Achilleos, H. Kasap, and E. Reisner, 'Photocatalytic hydrogen generation coupled to pollutant utilisation using carbon dots produced from biomass', *Green Chem.*, vol. 22, no. 9, pp. 2831–2839, 2020, doi: 10.1039/D0GC00318B.
17. E. Hosseini Koupaie, S. Dahadha, A. A. Bazyar Lakeh, A. Azizi, and E. Elbeshbishy, 'Enzymatic pretreatment of lignocellulosic biomass for enhanced biomethane production-A review', *Journal of Environmental Management*, vol. 233, pp. 774–784, Mar. 2019, doi: 10.1016/j.jenvman.2018.09.106.
18. D. M. A. Crista, A. El Mragui, M. Algarra, J. C. G. Esteves Da Silva, R. Luque, and L. Pinto Da Silva, 'Turning Spent Coffee Grounds into Sustainable Precursors for the Fabrication of Carbon Dots', *Nanomaterials*, vol. 10, no. 6, p. 1209, Jun. 2020, doi: 10.3390/nano10061209.
19. Z. Hu, X.-Y. Jiao, and L. Xu, 'The N,S co-doped carbon dots with excellent luminescent properties from green tea leaf residue and its sensing of gefitinib', *Microchemical Journal*, vol. 154, p. 104588, May 2020, doi: 10.1016/j.microc.2019.104588.
20. J. R. Bhamore, S. Jha, R. K. Singhal, T. J. Park, and S. K. Kailasa, 'Facile green synthesis of carbon dots from Pyrus pyrifolia fruit for assaying of Al3+ ion via chelation enhanced fluorescence mechanism', *Journal of Molecular Liquids*, vol. 264, pp. 9–16, Aug. 2018, doi: 10.1016/j.molliq.2018.05.041.
21. P. D., L. Singh, A. Thakur, and P. Kumar, 'Green synthesis of glowing carbon dots from Carica papaya waste pulp and their application as a label-freechemo probe for chromium detection in water', *Sensors and Actuators B: Chemical*, vol. 283, pp. 363–372, Mar. 2019, doi: 10.1016/j.snb.2018.12.027.
22. R. Atchudan, T. N. J. I. Edison, S. Perumal, N. Muthuchamy, and Y. R. Lee, 'Hydrophilic nitrogen-doped carbon dots from biowaste using dwarf banana peel for environmental and biological applications', *Fuel*, vol. 275, p. 117821, Sep. 2020, doi: 10.1016/j.fuel.2020.117821.
23. C. Cheng, M. Xing, and Q. Wu, 'A universal facile synthesis of nitrogen and sulfur co-doped carbon dots from cellulose-based biowaste for fluorescent detection of Fe3+ ions and intracellular bioimaging', *Materials Science and Engineering: C*, vol. 99, pp. 611–619, Jun. 2019, doi: 10.1016/j.msec.2019.02.003.
24. R. Atchudan, T. N. J. I. Edison, D. Chakradhar, S. Perumal, J.-J. Shim, and Y. R. Lee, 'Facile green synthesis of nitrogen-doped carbon dots using Chionanthus retusus fruit extract and investigation of their suitability for metal ion sensing and biological applications', *Sensors and Actuators B: Chemical*, vol. 246, pp. 497–509, Jul. 2017, doi: 10.1016/j.snb.2017.02.119.
25. X. Yang, D. Wang, N. Luo, M. Feng, X. Peng, and X. Liao, 'Green synthesis of fluorescent N,S-carbon dots from bamboo leaf and the interaction with nitrophenol compounds', *Spectrochimica Acta Part A: Molecular and Biomolecular Spectroscopy*, vol. 239, p. 118462, Oct. 2020, doi: 10.1016/j.saa.2020.118462.
26. Z. Li *et al.*, 'A fluorescence probe based on the nitrogen-doped carbon dots prepared from orange juice for detecting Hg 2+ in water', *Journal of Luminescence*, vol. 187, pp. 274–280, Jul. 2017, doi: 10.1016/j.jlumin.2017.03.023.
27. A. M. Senol and E. Bozkurt, 'Facile green and one-pot synthesis of seville orange derived carbon dots as a fluorescent sensor for Fe3+ ions', *Microchemical Journal*, vol. 159, p. 105357, Dec. 2020, doi: 10.1016/j.microc.2020.105357.
28. Y. Man *et al.*, 'Starch fermentation wastewater as a precursor to prepare S,N-doped carbon dots for selective Fe(III) detection and carbon microspheres for solution decolorization', *Microchemical Journal*, vol. 159, p. 105338, Dec. 2020, doi: 10.1016/j.microc.2020.105338.
29. X.-Y. Jiao, L. Li, S. Qin, Y. Zhang, K. Huang, and L. Xu, 'The synthesis of fluorescent carbon dots from mango peel and their multiple applications', *Colloids and Surfaces A: Physicochemical and Engineering Aspects*, vol. 577, pp. 306–314, Sep. 2019, doi: 10.1016/j.colsurfa.2019.05.073.
30. S. K. Haghani, A. A. Ensafi, N. Kazemifard, and B. Rezaei, 'A Sensitive and Selective Optical Sensor Based on Molecularly Imprinting Technique Using Green Synthesized Carbon Dots for Determination of Trace Amount of Metronidazole', *IEEE SENSORS JOURNAL*, vol. 20, no. 21, p. 7, 2020.
31. A. Águas *et al.*, 'Natural establishment of Eucalyptus globulus Labill. in burnt stands in Portugal', *Forest Ecology and Management*, vol. 323, pp. 47–56, Jul. 2014, doi: 10.1016/j.foreco.2014.03.012.
32. K. Sebei, F. Sakouhi, W. Herchi, M. Khouja, and S. Boukhchina, 'Chemical composition and antibacterial activities of seven Eucalyptus species essential oils leaves', *Biol Res*, vol. 48, no. 1, p. 7, 2015, doi: 10.1186/0717-6287-48-7.

33. W. Kasprzyk, T. Świergosz, S. Bednarz, K. Walas, N. V. Bashmakova, and D. Bogdał, 'Luminescence phenomena of carbon dots derived from citric acid and urea – a molecular insight', *Nanoscale*, vol. 10, no. 29, pp. 13889–13894, Jul. 2018, doi: 10.1039/C8NR03602K.
34. R. M. S. Sendão *et al.*, 'Insight into the hybrid luminescence showed by carbon dots and molecular fluorophores in solution', *Phys. Chem. Chem. Phys.*, vol. 21, no. 37, pp. 20919–20926, Sep. 2019, doi: 10.1039/C9CP03730F.
35. Christé, Esteves da Silva, and Pinto da Silva, 'Evaluation of the Environmental Impact and Efficiency of N-Doping Strategies in the Synthesis of Carbon Dots', *Materials*, vol. 13, no. 3, p. 504, Jan. 2020, doi: 10.3390/ma13030504.
36. R. U. Ayres, B. de Constance, and F. Cede, 'Life cycle analysis: A critique', 1995.
37. S. Fernandes, J. C. G. Esteves Da Silva, and L. Pinto Da Silva, 'Life Cycle Assessment-Based Comparative Study between High-Yield and "Standard" Bottom-Up Procedures for the Fabrication of Carbon Dots', *Materials*, vol. 15, no. 10, p. 3446, May 2022, doi: 10.3390/ma15103446.
38. S. Fernandes, J. C. G. Esteves Da Silva, and L. Pinto Da Silva, 'Comparative life cycle assessment of high-yield synthesis routes for carbon dots', *NanoImpact*, vol. 23, p. 100332, Jul. 2021, doi: 10.1016/j.impact.2021.100332.
39. Ricardo. Sendão, M. D. V. M. D. Yuso, M. Algarra, J. C. G. Esteves Da Silva, and L. Pinto Da Silva, 'Comparative life cycle assessment of bottom-up synthesis routes for carbon dots derived from citric acid and urea', *Journal of Cleaner Production*, vol. 254, p. 120080, May 2020, doi: 10.1016/j.jclepro.2020.120080.
40. M. A. J. Huijbregts *et al.*, 'ReCiPe2016: a harmonised life cycle impact assessment method at midpoint and endpoint level', *Int J Life Cycle Assess*, vol. 22, no. 2, pp. 138–147, Feb. 2017, doi: 10.1007/s11367-016-1246-y.
41. Y.-M. Long, C.-H. Zhou, Z.-L. Zhang, Z.-Q. Tian, Y. Lin, and D.-W. Pang, 'Shifting and non-shifting fluorescence emitted by carbon nanodots', p. 4, 2012.
42. K. Wang, C. Geng, F. Wang, Y. Zhao, and Z. Ru, 'Urea-doped carbon dots as fluorescent switches for the selective detection of iodide ions and their mechanistic study', *RSC Adv.*, vol. 11, no. 44, pp. 27645–27652, 2021, doi: 10.1039/D1RA04558J.
43. Y. Liu, 'Green preparation of carbon dots from Momordica charantia L. for rapid and effective sensing of p -aminoazobenzene in environmental samples', *Environmental Research*, p. 8, 2021.
44. X. Gao, L. Wang, C. Sun, and N. Zhou, 'Research on Preparation Methods of Carbon Nanomaterials Based on Self-Assembly of Carbon Quantum Dots', *Molecules*, vol. 27, no. 5, p. 1690, Mar. 2022, doi: 10.3390/molecules27051690.
45. A. Tiwari *et al.*, 'High quantum yield carbon dots and nitrogen-doped carbon dots as fluorescent probes for spectroscopic dopamine detection in human serum', *J. Mater. Chem. B*, vol. 11, no. 5, pp. 1029–1043, 2023, doi: 10.1039/D2TB02188A.
46. A. B. Padasalagi and M. H. K. Rabinal, 'Controlled Emission of Carbon Quantum Dots Derived from Waste Silk Sericin', *Part & Part Syst Charact*, vol. 39, no. 8, p. 2200041, Aug. 2022, doi: 10.1002/ppsc.202200041.
47. A. F. Shaikh, M. S. Tamboli, R. H. Patil, A. Bhan, J. D. Ambekar, and B. B. Kale, 'Bioinspired Carbon Quantum Dots: An Antibiofilm Agents', *j nanosci nanotechnol*, vol. 19, no. 4, pp. 2339–2345, Apr. 2019, doi: 10.1166/jnn.2019.16537.
48. A. C. Ferrari and J. Robertson, 'Interpretation of Raman spectra of disordered and amorphous carbon', *Phys. Rev. B*, vol. 61, no. 20, pp. 14095–14107, May 2000, doi: 10.1103/PhysRevB.61.14095.
49. Y.-Y. Liu *et al.*, 'Photodegradation of carbon dots cause cytotoxicity', *Nat Commun*, vol. 12, no. 1, p. 812, Feb. 2021, doi: 10.1038/s41467-021-21080-z.
50. Y. Dong *et al.*, 'Carbon-Based Dots Co-doped with Nitrogen and Sulfur for High Quantum Yield and Excitation-Independent Emission', *Angewandte Chemie International Edition*, vol. 52, no. 30, pp. 7800–7804, 2013, doi: 10.1002/anie.201301114.
51. Y. Zhang *et al.*, 'Fluorescent probes for "off–on" highly sensitive detection of Hg2+ and L-cysteine based on nitrogen-doped carbon dots', *Talanta*, vol. 152, pp. 288–300, May 2016, doi: 10.1016/j.talanta.2016.02.018.
52. A. N. Emam, 'Cyto-toxicity, biocompatibility and cellular response of carbon dots–plasmonic based nano-hybrids for bioimaging', *RSC Advances*, p. 13, 2017.
53. Y. Li *et al.*, 'Large-scale direct pyrolysis synthesis of excitation-independent carbon dots and analysis of ferric (III) ion sensing mechanism', *Applied Surface Science*, vol. 538, p. 148151, Feb. 2021, doi: 10.1016/j.apsusc.2020.148151.